Article

Molecular Cell

NADP$^+$*-IDH* Mutations Promote Hypersuccinylation that Impairs Mitochondria Respiration and Induces Apoptosis Resistance

Graphical Abstract

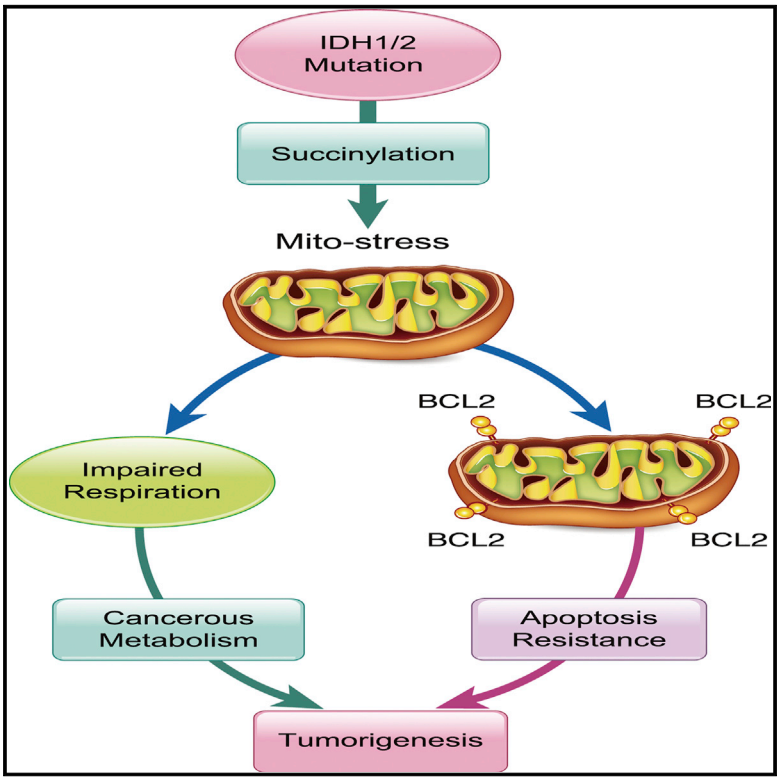

Authors

Feng Li, Xiadi He, Dingwei Ye, ..., Jianyuan Zhao, Wei Xu, Shimin Zhao

Correspondence

xuwei_0706@fudan.edu.cn (W.X.), zhaosm@fudan.edu.cn (S.Z.)

In Brief

NADP$^+$*-IDH* mutation-produced R-2-hydroxyglutarate induces mitochondrial hypersuccinylation that induces cancerous metabolism and apoptosis resistance. Relief of hypersuccinylation inhibits tumorigenic growth of *IDH* mutant-harboring cells. Thus, hypersuccinylation contributes to oncogenicity of R-2-hydroxyglutarate.

Highlights

- R-2HG competitively inhibits SDH and induces hypersuccinylation
- IDH1 mutations preferentially induce hypersuccinylation in mitochondria
- Hypersuccinylation impairs mitochondrial functions and induces apoptosis resistance
- Relief of hypersuccinylation inhibits oncogenic growth of hypersuccinylated cells

Accession Numbers

GSE73662

Li et al., 2015, Molecular Cell *60*, 661–675
November 19, 2015
http://dx.doi.org/10.1016/j.molcel.2015.10.017

Molecular Cell
Article

NADP$^+$*-IDH* Mutations Promote Hypersuccinylation that Impairs Mitochondria Respiration and Induces Apoptosis Resistance

Feng Li,[1,2,8,12] Xiadi He,[1,3,8,12] Dingwei Ye,[4,5,12] Yan Lin,[1,2,8] Hongxiu Yu,[2] Cuifang Yao,[1,2] Lei Huang,[1,3] Jianong Zhang,[1,3] Fang Wang,[2] Sha Xu,[1,2] Xiaohui Wu,[1,7] Lixia Liu,[9] Chen Yang,[9] Jiaqi Shi,[10] Xiaoyang He,[11] Jie Liu,[2,6,10] Yuanyuan Qu,[4,5] Fushen Guo,[1,2,3] Jianyuan Zhao,[1,3] Wei Xu,[1,2,8,*] and Shimin Zhao[1,2,3,6,8,*]
[1]State Key Lab of Genetic Engineering and the Obstetrics & Gynecology Hospital of Fudan University
[2]Institutes of Biomedical Sciences
[3]School of Life Sciences and Collaborative Innovation Center for Genetics and Development
[4]Department of Urology, Fudan University Shanghai Cancer Center
[5]Department of Oncology, Shanghai Medical College
[6]Institute of Digestive Medicine, Affiliated Huashan Hospital
[7]Institute of Developmental Biology and Molecular Medicine
Fudan University, Shanghai 200032, P.R. China
[8]State Key Laboratory of Biotherapy/Collaborative Innovation Center for Biotherapy, West China Hospital, Sichuan University, Chengdu 610041, P.R. China
[9]Institute of Plant Physiology and Ecology, Shanghai Institutes for Biological Sciences, Chinese Academy of Sciences, Shanghai 200031, P.R. China
[10]Department of Urology, Affiliated Hospital of Guiyang Medical College, Guiyang 550004, P.R. China
[11]Guizhou Cancer Hospital, Guiyang 550001, P.R. China
[12]Co-first author
*Correspondence: xuwei_0706@fudan.edu.cn (W.X.), zhaosm@fudan.edu.cn (S.Z.)
http://dx.doi.org/10.1016/j.molcel.2015.10.017

SUMMARY

Elucidating the tumorigenic mechanism of R-2-hydroxyglutarate (R-2HG) is critical for determining how *NADP*$^+$*-IDH* mutations cause cancer. Here we report that R-2HG induces cancerous metabolism and apoptosis resistance through promoting hypersuccinylation. By competitive inhibition of the mitochondrial tricarboxylic acid cycle enzyme succinate dehydrogenase (SDH), R-2HG preferentially induced succinyl-CoA accumulation and hypersuccinylation in the mitochondria. *IDH1* mutation-bearing glioma samples and cells were hypersuccinylated in the mitochondria. IDH1 mutation or SDH inactivation resulted in hypersuccinylation, causing respiration inhibition and inducing cancerous metabolism and mitochondrial depolarization. These mitochondrial dysfunctions induced BCL-2 accumulation at the mitochondrial membrane, leading to apoptosis resistance of hypersuccinylated cells. Relief of hypersuccinylation by overexpressing the desuccinylase SIRT5 or supplementing glycine rescued mitochondrial dysfunctions, reversed BCL-2 accumulation, and slowed the oncogenic growth of hypersuccinylated *IDH1* ^{R132C}-harboring HT1080 cells. Thus, R-2HG-induced hypersuccinylation contributes to the tumorigenicity of *NADP*$^+$*-IDH* mutations, suggesting the potential of hypersuccinylation inhibition as an intervention for hypersuccinylation-related tumors.

INTRODUCTION

Somatic mutations in the single arginine residue in the isocitrate dehydrogenase IDH1 or IDH2 have been identified in gliomas, acute myeloid leukemia, and other types of tumors (Amary et al., 2011; Parsons et al., 2008; Wang et al., 2013; Yan et al., 2009). *IDH1* and *IDH2* mutations gain them activities to reduce alpha-ketoglutarate (α-KG) to R-2-hydroxyglutarate (R-2HG) in the presence of NADPH (Dang et al., 2009). The proposed oncogenic mechanism of *IDH1* or *IDH2* mutations is accumulation of R-2HG, which is an analog of α-KG and inhibits α-KG-dependent dioxygenases (Xu et al., 2011). This mechanism is similar to the fumarate/succinate accumulation resulting from fumarate hydratase (*FH*) mutations (Isaacs et al., 2005) and the succinate accumulation resulting from succinate dehydrogenase *(SDH)* mutations (Selak et al., 2005). The α-KG-dependent dioxygenases, such as JmjC domain-containing histone demethylases and methylcytosine dioxygenase (Ten-Eleven-Translocation, TET), which mark 5-methylcytosine (5mC) for DNA demethylation, are particularly affected by such mutations. This hypothesis has been supported by observations that R-2HG decreased 5-hydroxylmethylcytosine (5hmC) levels in cells overexpressing TET (Xiao et al., 2012; Xu et al., 2011), and that the hypermethylator phenotype was associated with *IDH1*, *IDH2*, *FH*, and *SDH* mutations (Christensen et al., 2011; Killian et al., 2013; Letouzé et al., 2013; Lu et al., 2012; Turcan et al., 2012). Nevertheless,

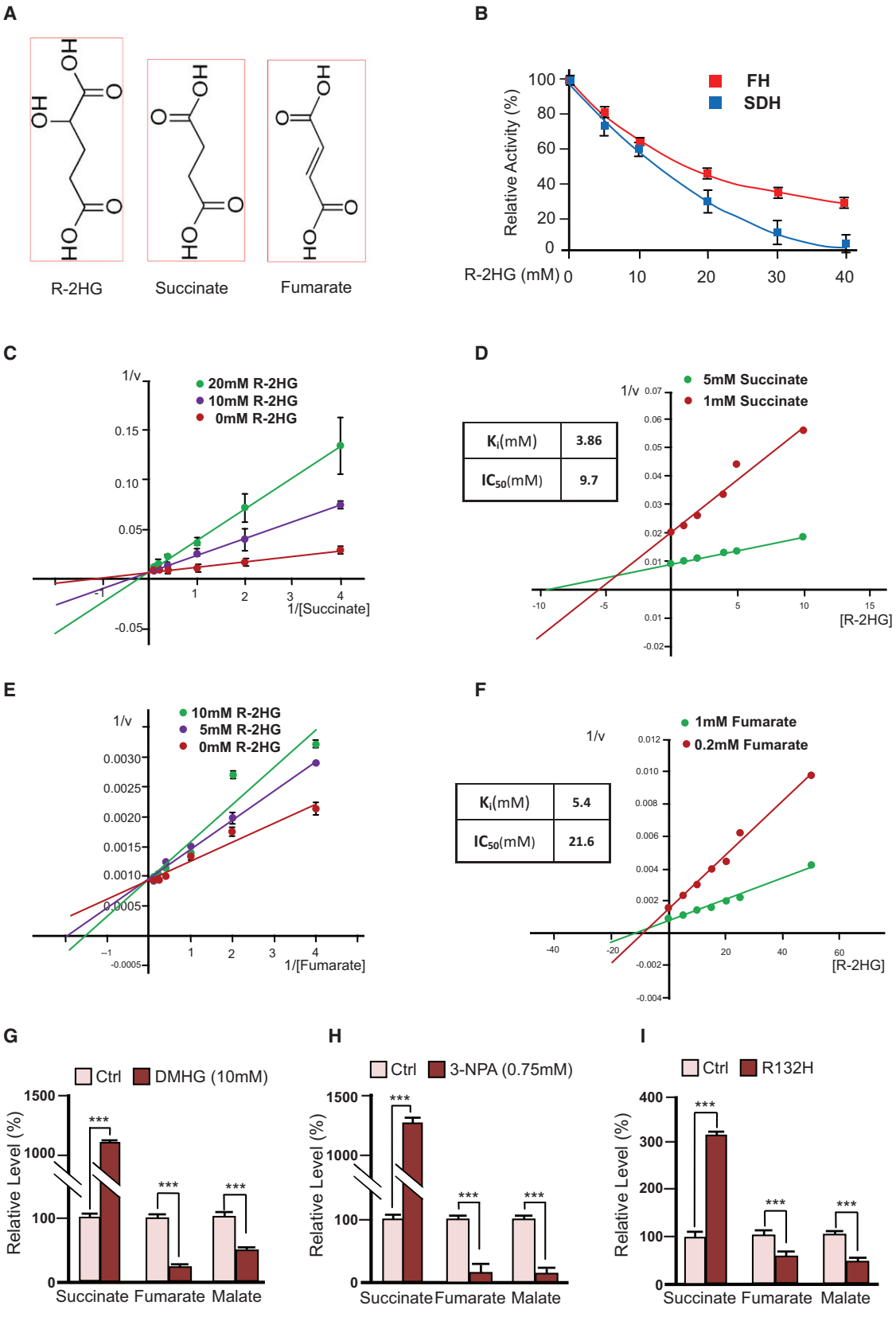

(legend on next page)

a direct causal mechanism is yet to be established between mutation-induced hypermethylation and tumorigenicity.

Although R-2HG alone is capable of promoting leukemogenesis (Losman et al., 2013) and inhibition of R-2HG production using the small molecule AGI5198 could curb tumor growth, no significant histone and DNA methylation decrease was resulted when R-2HG production was inhibited by AGI5198 (Rohle et al., 2013), indicating that the R-2HG-induced elevation of methylation may be dispensable for tumorigenicity, and highlighting alternative tumorigenic mechanisms of R-2HG. *IDH1/2* mutations induce dependence of the apoptosis inhibitor BCL-2 in acute myeloid leukemia (Chan et al., 2015), suggesting that the tumorigenic effect of *IDH1/2* mutations may include altered apoptosis.

Metabolites associated protein regulations including feedback inhibition, allosteric regulation, and posttranslational modification (PTM) (Li et al., 2013). Metabolite-derived PTMs are increasingly appreciated for their roles in physiological regulation because they are widespread. For example, lysine acetylation is known to regulate the functions of many proteins (Grunstein, 1997; Hirschey et al., 2010; Zhao et al., 2010). Lysine succinylation (hereafter referred to as succinylation) was recently identified as a particularly common and widespread PTM, whose level is regulated by the desuccinylase SIRT5 (Du et al., 2011; Park et al., 2013; Rardin et al., 2013; Zhang et al., 2011) in cells. However, the pathologic effects of either hyper- or hyposuccinylation remain largely unexplored. Succinylation employs succinyl-CoA to modify lysines (Du et al., 2011), and is also known to regulate the functions of its substrates (Zhang et al., 2011). Succinyl-CoA is an immediate upstream metabolite of succinate and fumarate, two known tricarboxylic acid (TCA) cycle oncometabolites, and is in equilibrium with succinate at interconversion free energies ($\Delta G'^{0}$) close to zero in isolated pig heart mitochondria (Nelson and Cox, 2008). Thus, succinate accumulation would be expected to significantly increase succinyl-CoA levels. Together, these facts have led to the hypothesis that hypersuccinylation would be induced in tumors with *FH* and *SDH* mutations. Notably, R-2HG is a structural analog of both succinate and fumarate and could serve as an inhibitor of both FH and SDH. Therefore, expression of *IDH1* or *IDH2* mutations in cells would cause FH and SDH inhibition via R-2HG accumulation, thereby simulating the effects of *SDH* and *FH* mutations to induce hypersuccinylation. In the current study, we examined whether and how *IDH1* and *IDH2* mutations promote cancer transformation by inducing hypersuccinylation.

RESULTS

R-2-HG Competitively Inhibits SDH and FH In Vitro

Since R-2HG is a structural analog of succinate and fumarate (Figure 1A), it would compete for the succinate- and fumarate-binding sites and inhibit activities of SDH and FH, respectively. This idea was tested by using recombinant FH and purified SDH complex in mitochondria from human embryonic kidney HEK293T cells. When succinate was used at physiologic concentrations of approximately 1 mM (Bennett et al., 2009), R-2HG dose-dependently inhibited SDH activity (Figure 1B). Kinetic analysis revealed a competitive mode for R-2HG to inhibit SDH (Figure 1C), and confirmed that R-2HG binds to the succinate-binding site of SDH. Moreover, Dixon plot analysis showed that the K_i of R-2HG was 3.86 mM, and the IC_{50} value at 1 mM succinate for R-2HG on SDH was 9.7 mM (Figure 1D). These represent SDH and can be inhibited at R-2HG concentrations that are readily available in *$NADP^+$-IDH* mutation-bearing cancer cells, which accumulate R-2HG up to 5–35 mM (Dang et al., 2009; Xu et al., 2011).

When fumarate was used at 1 mM, the specific activity of FH was dose-dependently inhibited by R-2HG (Figure 1B). Lineweaver-Burk plots revealed that R-2HG competitively inhibited FH (Figure 1E). Moreover, the K_i of R-2HG was 5.40 mM, and the IC_{50} value at 1 mM fumarate for R-2HG on FH was 21.6 mM (Figure 1F). These results demonstrated that while R-2HG inhibited FH and SDH with similar potency, the same concentration of R-2HG resulted in stronger inhibition to SDH when the substrate concentrations of FH and SDH were near physiological concentrations.

R-2HG Inhibits SDH More Completely Than FH in Cultured Cells

To understand how SDH and FH are separately inhibited by R-2HG in cells, we detected the concentrations of succinate (the substrate for SDH), fumarate (the product of SDH and the substrate for FH), and malate (the product of FH), using different approaches for manipulating R-2HG levels. Treatment of 10 mM membrane-permeable R-2HG ester dimethyl-R-2HG (DMHG) (Xiao et al., 2012) elevated cellular R-2HG levels in U87MG glioblastoma cells from 2 μM to 6.8 mM (see Figure S1 and Table S1 available online), increased cellular succinate levels by more than 10-fold, but decreased cellular fumarate and malate levels by more than 50% (Figure 1G). These results showed that R-2HG inhibits SDH more efficiently in cells. Supporting this notion, SDH inhibitor 3-nitropropionic acid (3-NPA) treatment

Figure 1. R-2HG Accumulates Succinate by Inhibiting SDH

(A) Chemical structures of fumarate, succinate, and 2HG.

(B) Relative specific activities of recombinant FH and the purified SDH complex were assayed in the presence of indicated concentrations of R-2HG when 1 mM fumarate or succinate was used as substrate. All activities were normalized to those of without R-2HG in the reaction. Error bars are ± SD.

(C) Lineweaver-Burk plots showed that R-2HG competitively inhibited SDH. Error bars are ± SD.

(D) The inhibitory constant (K_i) was calculated from a Dixon plot; the IC_{50} was calculated at a succinate concentration of 1 mM.

(E) Lineweaver-Burk plots showed that R-2HG competitively inhibited FH. Error bars are ± SD.

(F) Dixon plot derived K_i and IC_{50}. For IC_{50}, fumarate concentration was 1 mM.

(G–I) Relative levels of cellular succinate, fumarate, and malate were compared between HEK293T cells and (G) HEK293T cells treated with 10 mM DMHG, (H) HEK293T cells treated with 0.75 mM NPA, and (I) HEK293T cells overexpressing $IDH1^{R132H}$. Levels of metabolites in HEK293T cells (Table S1) were set as 100%. Error bars are ± SD (n = 3).

See also Figure S1 and Table S1.

to cells resulted in similar changes to these metabolites (Figure 1H). Moreover, *IDH1*^{R132H} overexpression in HEK293T cells increased cellular succinate levels by 220% and decreased fumarate and malate levels by approximately 50% (Figure 1I), and confirmed that *IDH1*^{R132H} expression results in SDH inhibition and the accumulation of succinate in cells.

SDH Inactivation Induces Succinyl-CoA Accumulation and Hypersuccinylation

Treatment by dimethyl-succinate (DMS) caused an approximately 4-fold increase in succinyl-CoA levels and induced hypersuccinylation, as detected with an in house-designed anti-pan-succinyllysine antibody (α-SucK) (Figure S2), in U87MG cells (Figure 2A). Moreover, inactivating SDH by depleting the SDHA or SDHB subunits of the SDH complex using small hairpin RNAs (shRNAs) resulted in 500% and 290% increases in succinyl-CoA levels and hypersuccinylation (Figure 2B), respectively. Furthermore, inhibiting SDH using 750 μM 3-NPA led to a 210% increase of succinyl-CoA and hypersuccinylation (Figure 2C) in HEK293T cells. These results confirmed that SDH inactivation would induce hypersuccinylation by accumulating succinyl-CoA.

Succinyl-CoA has been reported to spontaneously modify lysine (Colak et al., 2013; Wagner and Payne, 2013; Weinert et al., 2013). We confirmed this by incubating synthetic N terminus blocked peptides with succinyl-CoA at a 1:2 molar ratio and found that only the peptides containing lysine, but not those devoid of lysine, were succinylated by succinyl-CoA (Figure 2D). Moreover, incubation of succinyl-CoA with bovine serum albumin (BSA) resulted in dose-dependent BSA succinylation (Figure 2E). These results suggest that the levels of succinyl-CoA determine levels of succinylation.

NADP$^+$-IDH Mutations Induce Hypersuccinylation by Producing R-2HG

DMHG treatments caused an elevation of succinyl-CoA and hypersuccinylation in both U87MG cells (Figure 3A) and primary mouse hepatocytes (Figure 3B), and confirmed that R-2HG inhibits SDH and induces hypersuccinylation. Notably, R-2HG treatment had negligible effects on malonylation and glutarylation (Figure S3A), the other substrates of SIRT5 besides succinylation (Du et al., 2011), and showed that R-2HG specifically affects succinylation levels.

IDH1^{R132H}, but not a catalytically inactive and R-2HG-nonproducing *IDH1*^{K212Q} mutant (Figure S3B), stably overexpressed at levels comparable to endogenous *IDH1* (Figures S3C) resulted in a 280% increase in cellular succinyl-CoA levels and hypersuccinylation (Figures 3C). Moreover, inhibiting the oxidative decarboxylation activity of IDH1 with oxalomalate (Zhao et al., 2009) failed to induce hypersuccinylation in U87MG cells (Figure 3D). Hypersuccinylation was also prevented by the inhibition of R-2-HG production by IDH1^{R132H} with AGI5198 (Rohle et al., 2013) when *IDH1*^{R132H} was ectopically expressed in U87MG cells (Figure 3E). These results conclusively showed that R-2HG production, rather than the loss of catalytic activity in IDH1^{R132H}, induces hypersuccinylation. Consistently, overexpression of *IDH2*^{R172M}, another R-2-HG-producing *NADP$^+$-IDH* mutant that promotes cancer (Figueroa et al., 2010), induced hypersuccinylation in U87MG cells (Figure 3F).

IDH1 Mutation-Bearing Gliomas and IDH1^{R132H}-Expressing Cells Are Preferentially Hypersuccinylated in the Mitochondria

To test the pathological relevance of hypersuccinylation, we collected and sequenced glioma samples for *IDH1* mutations. The identified ten *IDH1* mutation-bearing samples were matched with an equal number of randomly selected *IDH1* wild-type glioma samples (Table S2) and were subjected to immunohistochemistry (IHC) analysis for succinylation levels. *IDH1* mutation-bearing glioma samples were more highly succinylated than wild-type *IDH1* samples (Figures 4A and S4A), and confirmed that hypersuccinylation is induced in *IDH1*-mutation-bearing cancer cells. Notably, although succinylation signals were detected throughout the cells, intense succinylation signals were found to localize to the mitochondria (Figure 4B), suggesting that *IDH1* mutations preferentially induce hypersuccinylation in the mitochondria. Moreover, the succinylation signals of R-2HG-producing *IDH1*^{R132C}-mutation bearing fibrosarcoma HT1080 cells (Jin et al., 2012; Rohle et al., 2013) were also found to overlap with mitochondrial signals (Figure 4C). Furthermore, stable expression of *IDH1*^{R132H} (Figure S4B) in U87MG cells enhanced the global succinylation and concentrated succinylation to the mitochondria (Figure 4D). These findings provided direct evidence that *IDH1*^{R132H} preferentially induces hypersuccinylation in the mitochondria.

Compartmentalized High Succinyl-CoA Levels Cause More Severe Hypersuccinylation in the Mitochondria

The fact that succinyl-CoA is produced and constrained within the mitochondria may explain the preferred hypersuccinylation in the mitochondria. Indeed, the succinylation levels of mitochondrial proteins from HEK293T cells were more highly succinylated than those of cytosolic and nuclear proteins (Figure 4E), which confirmed the hypothesis that mitochondrial proteins are highly succinylated. Moreover, knockdown of *SDHB* by *shRNA* significantly increased the succinylation levels of mitochondrial proteins but barely increased the succinylation levels of cytosolic and nuclear proteins (Figure 4E). These results verified that SDH inactivation induced more severe proteins hypersuccinylation in the mitochondria than in cytosol and nuclear. Consistent with the observation that *IDH1*^{R132H} overexpression inactivated SDH, overexpression of *IDH1*^{R132H} in U87MG cells significantly increased the levels of succinylation in mitochondrial proteins, but only mildly increased the levels of succinylation in cytosolic and nuclear proteins (Figure 4F). Collectively, these results showed that the events that inactivate SDH, such as overexpressing *IDH1*^{R132H}, preferentially promote hypersuccinylation in the mitochondria.

Hypersuccinylation Regulates Histones Methylation, the Gene Expression and Activities of Metabolic Enzymes

We examined hypersuccinylation effects in the nuclei, cytosol, and mitochondria, respectively. *IDH1*^{R132H} overexpression increased succinylation levels of histones (Figure 5A);

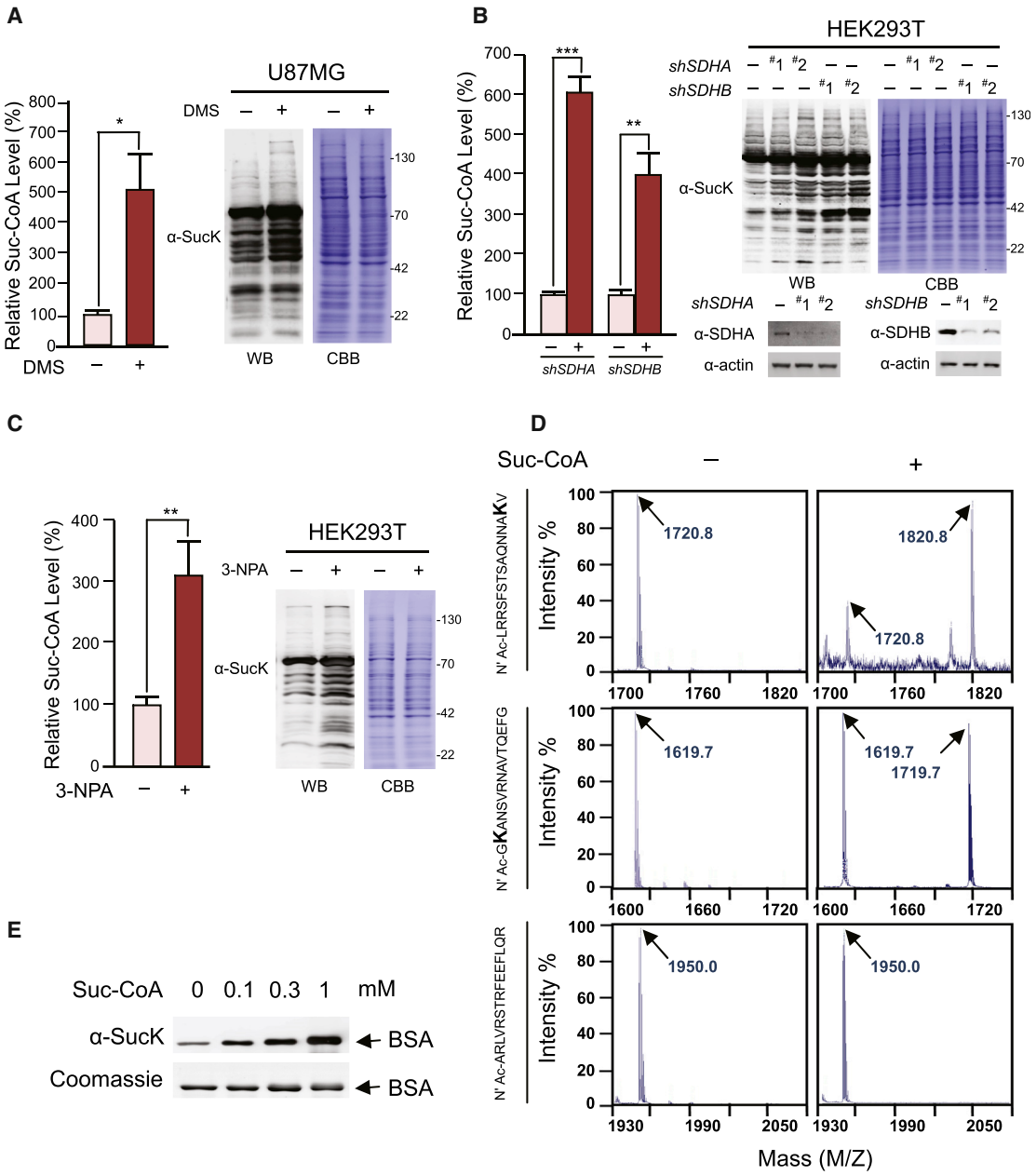

Figure 2. Inactivation of SDH Induces Hypersuccinylation by Accumulating Succinate and Succinyl-CoA

(A) DMS was added to the culture media to reach a final concentration of 10 mM. The succinyl-CoA levels (left, n = 4; error bars are ± SD) and succinylation levels of treated and untreated cells were compared.

(B) *SDHA* or *SDHB* was knocked down by independent *shRNA*s (knockdown efficiencies were confirmed, right bottom). The succinyl-CoA levels of *shRNA* #2 knockdown and control cells were determined by GC-MS (left, n = 4; error bars are ± SD). Succinylation levels of knockdown and control cells were determined by western blot (right, upper). Succinylation levels were normalized by proteins levels stained with Coomassie brilliant blue (CBB).

(C) 3-NPA was added to the culture media at a final concentration of 0.75 mM. The succinyl-CoA levels (left, n = 4; error bars are ± SD) and succinylation levels (right) of treated and untreated cells were compared.

(D) The modification products between synthetic N terminus blocked peptides and succinyl-CoA were analyzed by MS, and *m/z* values were indicated by arrows.

(E) The succinylation levels of BSA that was incubated with indicated concentrations of succinyl-CoA were determined.

See also Figure S2 and Table S1.

overexpression of SIRT5 reversed the H3K4me1, H3K36me2, and H3K36me3 hypermethylation induced by DMHG treatment (Figure 5B); *IDH1*^{R132H} overexpression or *SIRT5* knockdown (Figure S5A) resulted in similar changes in gene expression (Figures 5C, S5B, and S5C), and *IDH1*^{R132H} overexpression-induced gene expression alterations were partially

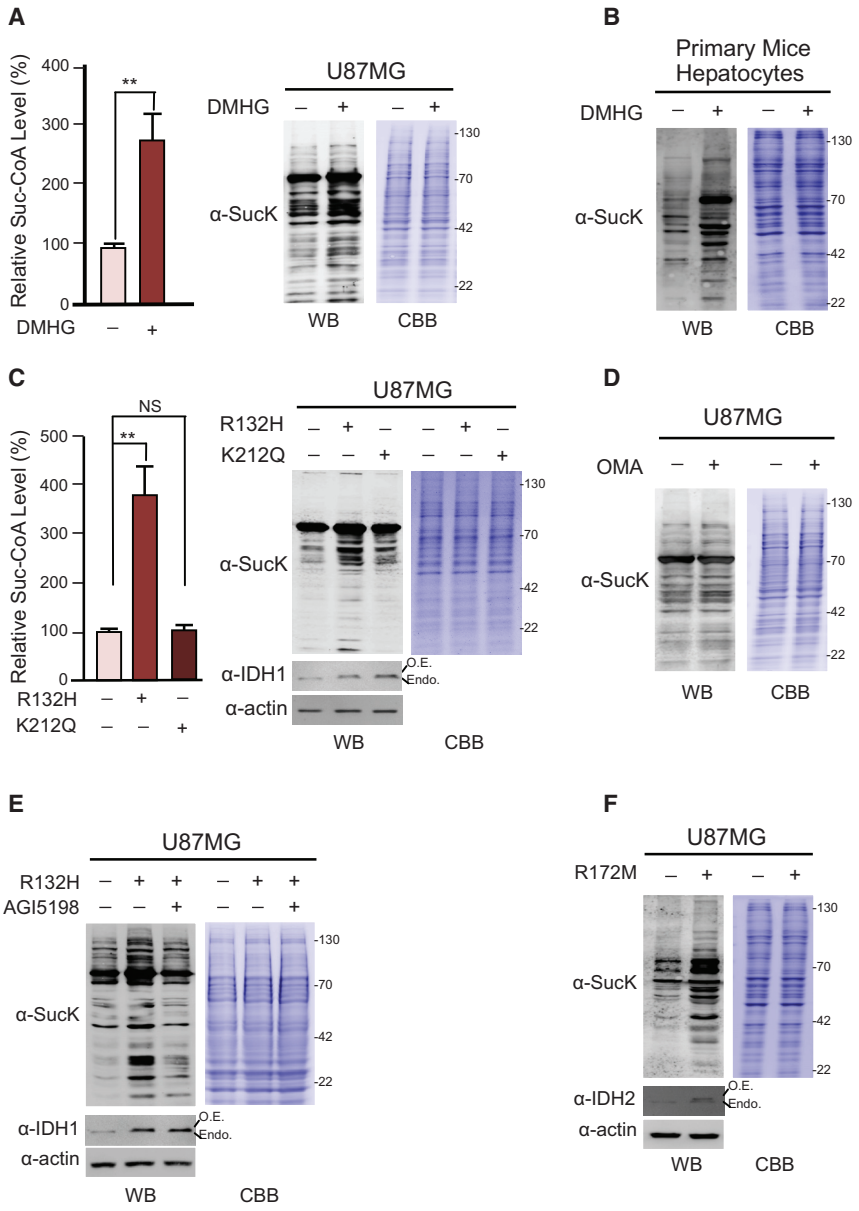

Figure 3. NADP$^+$-*IDH* Mutations Induce Hypersuccinylation by Accumulating R-2HG

(A) DMHG was added to the culture media to reach a final concentration of 10 mM. The succinyl-CoA levels (left, n = 4; error bars are ± SD) and the succinylation levels of treated and untreated cells were determined.

(B) The succinylation levels of 10 mM DMHG treated and untreated primary mice hepatocytes were determined. Cells were harvested after 24 hr of treatment.

(C) IDH1^{R132H} (R132H) and IDH1^{K212Q} (K212Q) were each overexpressed (O.E.) at levels comparable to that of endogenous (Endo.) level, and the succinyl-CoA levels (left, n = 4; error bars are ± SD) and succinylation levels (right) of IDH1 overexpressing and control cells were determined.

(D) The succinylation levels of 5 mM oxalomalate (OMA) treated and control cells were determined after 10 hr of treatment.

(E) R132H was overexpressed in cells cultured in the presence or absence of AGI5198 (1.5 μM). The level of succinylation from control cells and R132H overexpressing cells with or without AGI5198 treatment were compared 48 hr after transfection.

(F) The succinylation levels of IDH2^{R172M} (R172M) overexpressing and control cells were determined 48 hr after R172M transfection.

See also Figure S3.

reversed by SIRT5 overexpression (Figures 5D, S5B, and S5D) in U87MG cells. Moreover, knockdown of *SIRT5* or *IDH1*^{R132H} overexpression in HEK293T cells increased succinylation levels but inhibited the specific activities of cytosolic phosphoglycerate kinase (PGK) and IDH1 (Figures 5E, 5F, S5E, and S5F). Moreover, in vitro SIRT5 treatment of these two enzymes purified from *IDH1*^{R132H}-expressing HEK293T cells enhanced their activity by 22%–63% (Figure 5G). Further, affinity enrichment followed by mass spectrometry (MS) analysis (Adam et al., 2011; Ooi et al., 2011) identified succinylation sites in PDHA1, the catalytic subunit of the pyruvate dehydrogenase complex, SDHB, and cytochrome *c* oxidase (COX) (Figure S5G). Estimated by peptide counting, *IDH1*^{R132H} overexpression increased succinylation levels of identified sites from around 20% to about 60% (Figure S5H). Lysine-to-glutamate switches at the succinylation site to mimic succinylation resulted in decreases in the specific activities of all enzymes (Figure 5H), and suggested that succinylation negatively regulates activities of these enzymes. Confirming this notion, *IDH1*^{R132H} overexpression that decreased the specific activities of all three enzymes was reversed by SIRT5 overexpression in U87MG cells (Figure 5I). Collectively, these results showed that hypersuccinylation, although induced at different levels in distinct compartments of cells, exerts broad impacts in functions of nuclear, cytosolic, and mitochondrial proteins.

Hypersuccinylation Depolarizes the Mitochondria and Induces Cancerous Metabolism

Inactivation of SDH and COX, components of the mitochondrial electron transport chain, by hypersuccinylation implied that hypersuccinylation impairs oxidative phosphorylation. In line with this hypothesis, the oxygen consumption rates (OCRs) of primary mouse hepatocytes were decreased by 10 mM DMS or 5 mM DMHG treatment; but SIRT5 overexpression rendered the OCR of mouse hepatocytes resistant to DMHG (Figure 5J) and DMS (Figure S5I) treatment. Notably, different from reported results showing that *SIRT5* knockout enhanced complex II function and OCR in liver mitochondria from *Sirt5*-knockout *c57/129*

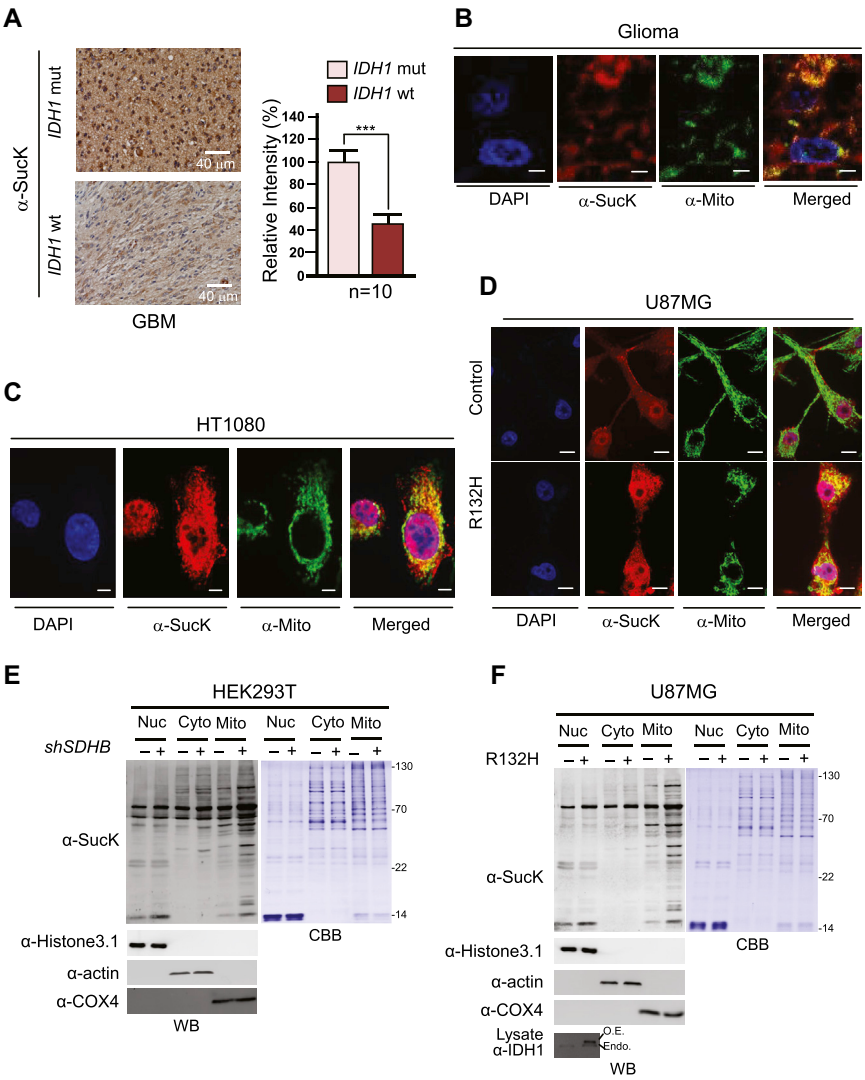

Figure 4. *NADP*$^+$*-IDH* Mutations Preferentially Induce Mitochondrial Hypersuccinylation

(A) Representative images of IHC (left) and quantification (right, n = 10; error bars are ± SD) of succinylation in *IDH1* mutation-bearing and in *IDH1* wild-type glioma samples.

(B) Overlap of succinylation signals with mitochondria signals in *IDH1* mutation-bearing glioma samples (scale bar, 5 μm).

(C) Overlap of succinylation signals with mitochondria signals in *IDH1*^{R132C} mutant-bearing HT1080 cells (scale bar, 10 μm).

(D) The changes in the intensity of succinylation in the mitochondria and in other compartments of the cells were compared between control and stably R132H-expressing cells (scale bar, 10 μm).

(E) Nuclear, cytosolic, and mitochondria fractions and *SDHB*-knockdown HEK293T cells were obtained, and the levels of succinylation between fractions of control cells and *SDHB*-knockdown cells were compared. The purity of each fraction was confirmed by its specific marker.

(F) R132H was overexpressed. Cytosolic, nuclear, and mitochondria fractions of *IDH1* mutant-expressing and control cells were obtained. The levels of succinylation among cytosolic, nuclear, and mitochondrial proteins of each cell were compared.

See also Figure S4 and Table S2.

mice (Park et al., 2013), SIRT5 depletion inhibited, rather than improved, the OCR of MEFs of *c57/129* mice in the present study (Figure 5K).

Overexpression of IDH1^{R132H} in U87MG cells increased lactate production (Figure 5L) and the ratio of pyruvate/citrate (Figure 5M); however, these effects were reversed by SIRT5 overexpression. These results showed that IDH1^{R132H} overexpression induces the Warburg effect and inhibition of hypersuccinylation relief it. Notably, SIRT5 knockdown caused decreased lactate production (Figure S5J), suggesting other SIRT5-controlled PTMs, such as malonylation and glutarylation, may exert different effects on metabolism (Nishida et al., 2015).

As further support that hypersuccinylation impairs mitochondrial functions, mitochondrial membrane potential was decreased by *shRNA*-induced knockdown of *SIRT5* (Figure S5K), as detected by both flow cytometry and immunofluorescence (Figures 5N and S5L). Moreover, *IDH1*^{R132H} overexpression caused a decrease in mitochondria membrane potential, which was rescued by SIRT5 overexpression (Figures 5O and S5M).

Furthermore, depletion of both the ADP-forming and GDP-forming succinyl-CoA synthetases by small interfering RNAs (siRNAs) in HEK293T cells increased succinyl-CoA and succinylation levels, but decreased succinate levels (Figures S5N–S5P) and mitochondrial membrane potential (Figure 5P), suggesting that hypersuccinylation alone is sufficient to depolarize the mitochondria. Collectively, these results confirmed that *IDH1* mutations induce mitochondrial depolarization and respiration impairment.

Hypersuccinylation Induces the Mitochondria Membrane Localization of BCL-2 and Promotes Apoptosis Resistance

Mitochondrial stress often results in apoptosis (Maloyan et al., 2005). The apoptosis-promoting effect of *IDH1* mutation was confirmed by the fact that overexpression of *IDH1*^{R132H} in U87MG cells mildly increased their apoptosis rate (Figure 6A), and conversely, knockout of *IDH1*^{R132C} in the *IDH1*^{R132C} mutation-harboring HT1080 cells reduced their apoptosis rate (Figure 6B). However, these results contradict with the fact that *IDH1* mutations are tumorigenic, as apoptosis generally prevents tumor development. To explain this apparent conflict, we speculated that *IDH1* mutation-harboring cells may acquire the ability to survive apoptotic stimuli. Indeed, *IDH1*^{R132H} overexpression slightly increased the apoptosis rate of U87MG cells but diminished the response of apoptosis rates of cells to apoptosis

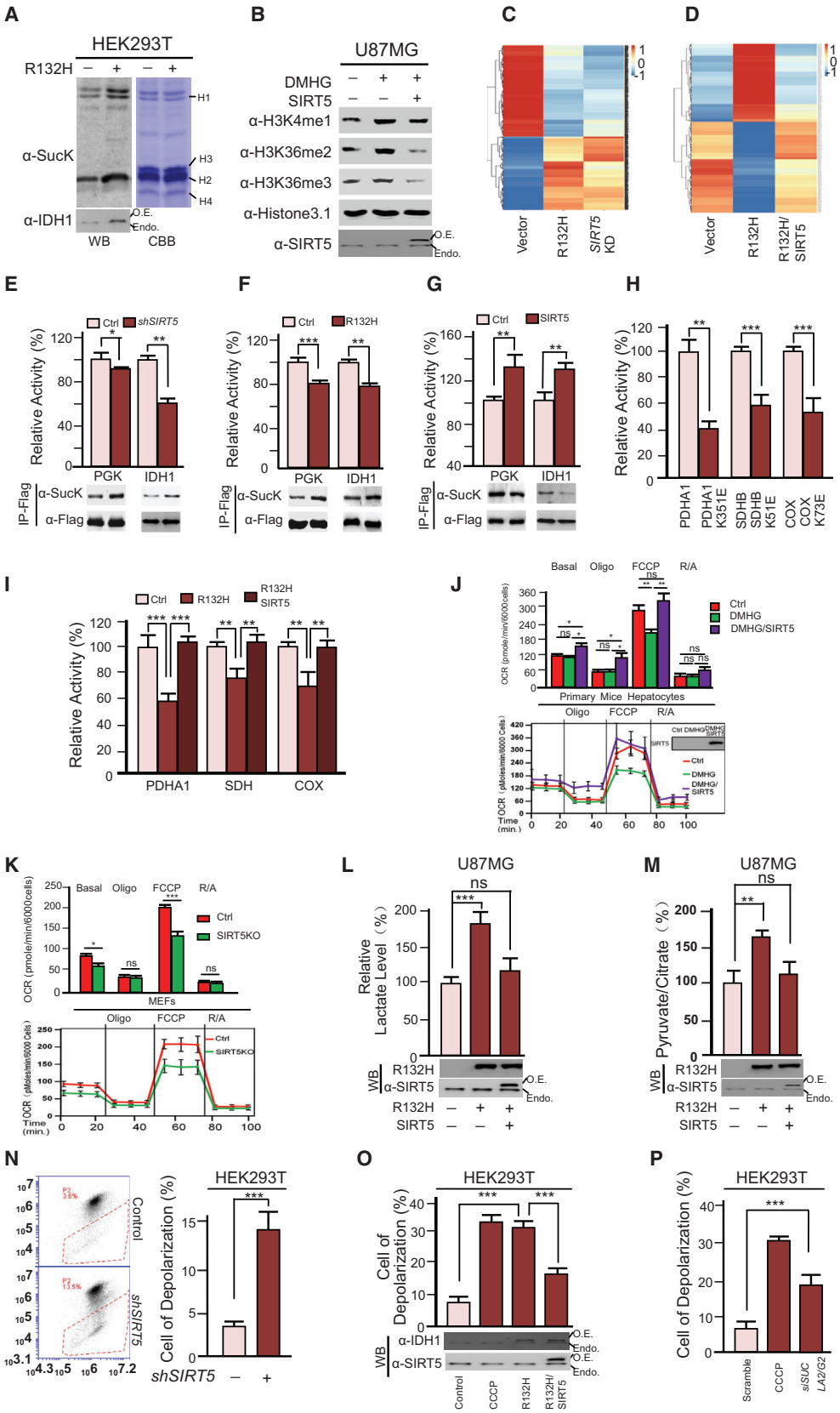

(legend on next page)

inducer sodium butyrate as well as physiological stresses such as low glucose and hypoxia (Figure 6C), demonstrating that *IDH1*^{R132H} overexpression confers apoptosis resistance to cells. This was in line with both *IDH1*^{R132C} knockout (Ma et al., 2015) and SIRT5 overexpression sensitizing HT1080 cells to stress-induced apoptosis (Figures 6D and 6E). Moreover, *SDHB* knockdown also induced apoptosis resistance in HEK293T cells in a *SIRT5* overexpression-reversible manner (Figure 6F). Together, these results confirmed that hypersuccinylation results in apoptosis resistance in cells.

Since the mitochondrial membrane potential is maintained, at least partially, by BCL-2 family proteins (Harris and Thompson, 2000), and *IDH1/2* mutations were found to induce BCL-2 dependence in acute myeloid leukemia (Chan et al., 2015), we tested the role of BCL-2 in hypersuccinylation-induced apoptosis resistance. *IDH1*^{R132H}-overexpressing U87MG cells treated with ABT-199, a specific BCL-2 inhibitor, showed more severe apoptosis than U87MG cells, whereas overexpression of BCL-2 in U87MG cells decreased the ABT-199-induced difference in apoptosis (Figure 6G). Similarly, ABT-199 treatment induced more severe apoptosis in *SDHB*-knockdown HEK293T cells than in HEK293T cells, whereas BCL-2 overexpression inhibited this difference (Figure 6H). These results confirmed an indispensable role of BCL-2 in hypersuccinylation-induced apoptosis resistance.

Mechanistically, neither *IDH1*^{R132H} overexpression in U87MG cells nor *SDHB* knockdown in HEK293T cells increased total BCL-2 levels (Figures 6I and 6J), in line with the previous observation that *IDH1*^{R132H} overexpression did not alter total cellular BCL-2 levels (Chan et al., 2015). However, both manipulations induced the accumulation of BCL-2 in the mitochondrial membrane (Figures 6I and 6J). Moreover, *SIRT5* knockdown also promoted BCL-2 to the mitochondrial membrane (Figure 6K). Collectively, these results suggest that hypersuccinylation recruits BCL-2 to the mitochondrial membrane, an event known to prevent apoptosis and induce cancers (Zamzami et al., 1996).

Although *SIRT5* overexpression in HT1080 cells (Figure 6E) and *SDHB*-knockdown HEK293T cells (Figure 6F) abolished their apoptosis resistance, overexpression of a mitochondria localization-defective but functional (Figures S6A and S6B) mutant, SIRT5$^{\Delta 50}$, failed to do so. These are consistent with that overexpression of SIRT5, but not SIRT5$^{\Delta 50}$, reversed the mitochondria membrane accumulation of BCL-2 (Figure 6L). Together, these results demonstrated that mitochondria hypersuccinylation is the major contributor of the observed apoptosis resistance of cells.

Relief of Hypersuccinylation Slows the Oncogenic Growth of HT1080 Cells

The tumor-promoting effects of *IDH1* mutation-induced hypersuccinylation were demonstrated. Stable overexpression of SIRT5 slowed the growth of HT1080 cells that harbor the R-2HG-producing *IDH1*^{R132C} mutation (Jin et al., 2012), but not HEK293T cells (Figure 7A), consistent with AGI5198 treatment decreasing succinylation in HT1080 cells (Figure 7B), and implying that R-2HG-driven hypersuccinylation promotes the oncogenic growth of HT1080 cells. Moreover, overexpression of SIRT5, but not catalytic inactive SIRT5^{R105M}, effectively decreased succinylation levels in HT1080 cells (Figure 7C). This, together with the fact that SIRT5-expressing HT1080 cell-produced xenografts were 75% smaller than those of HT1080 cells (Figure 7D), supported the idea that hypersuccinylation promotes the oncogenic growth of HT1080 cells.

Succinyl-CoA can be condensed with glycine by D-aminolevulinate synthase 1 to form 5-aminolevulinate and enter the heme

Figure 5. Hypersuccinylation Regulates Nuclear and Cytosolic Functions and Impairs Mitochondrial Functions

(A) Succinylation levels of isolated control histones and *IDH1*^{R132H}-expressing histones were determined.

(B) Cells with and without SIRT5 overexpression were treated with DMHG. Histone methylation levels were measured.

(C) Gene transcription levels of cells of U87MG, U87MG expressing *IDH1*^{R132H}, and U87MG with *SIRT5* knockdown by *shRNA* were analyzed by microarray and compared.

(D) Gene transcription levels of cells of U87MG, U87MG expressing *IDH1*^{R132H}, and U87MG coexpressing *IDH1*^{R132H} and *SIRT5* were analyzed by microarray and compared.

(E and F) The relative specific activities (upper panels, n = 4; error bars are ± SD) and succinylation levels (bottom panels) of Flag-tagged PGK and IDH1 in HEK293T cells. Comparisons were made between (E) control and *SIRT5* knockdown cells and (F) control and *IDH1*^{R132H}-expressing cells.

(G) Enzymes purified from *IDH1*^{R132H}-expressing HEK293T cells were treated with SIRT5 in vitro. The activities of both untreated and treated enzymes were determined and compared. All activities were normalized to that of untreated enzymes. Error bars, ± SD.

(H) Relative specific activities of PDHA1, SDH, and COX lysine-to-glutamate mutants were determined. All activities were normalized to those of wild-type enzymes. Error bars: ± SD.

(I) The relative specific activities of PDHA1, SDH, and COX overexpressed and purified from U87MG, *IDH1*^{R132H}-expressing U87MG, and *IDH1*^{R132H}/*SIRT5*-coexpressing U87MG cells were compared. Error bars, ± SD.

(J) Oxygen consumption rates (OCR) were detected (bottom) for untransfected and SIRT5-transfected (>80 efficiency) primary mouse hepatocytes that were treated by DMHG. OCR under oligomycin, carbonyl cyanide-m-chlorophenylhydrazone (FCCP), and antimycin A/rotenone treatments, respectively, at times indicated were obtained. Error bars, ± SEM.

(K) OCR of MEFs of c57/129 mice and *Sirt5* knockout c57/129 mice were detected (bottom) and quantified (upper). Error bars, ± SEM.

(L and M) Cellular lactate, pyruvate, and citrate levels were detected for U87MG, *IDH1*^{R132H}-expressing U87MG, and SIRT5/ *IDH1*^{R132H} coexpressing U87MG cells. Lactate (L) and pyruvate/citrate ratios (M) among these cells were compared. Error bars, ± SD.

(N) Mitochondrial membrane potential was probed by JC-1 staining. Percentages of depolarized cells in HEK293T and in *SIRT5*-knockdown HEK293T cells were detected by flow cytometry. Error bars, ± SD.

(O) JC-1 staining of cell depolarization for HEK293T, *IDH1*^{R132H}-expressing HEK293T, and *SIRT5*/*IDH1*^{R132H} coexpressing HEK293T cells; CCCP-treated cells were used as a positive control. Error bars, ± SD.

(P) The percentages of depolarized HEK293T and *SUCLA2*/*G2* double-knockdown HEK293T cells were determined. Error bars, ± SD.

See also Figure S5.

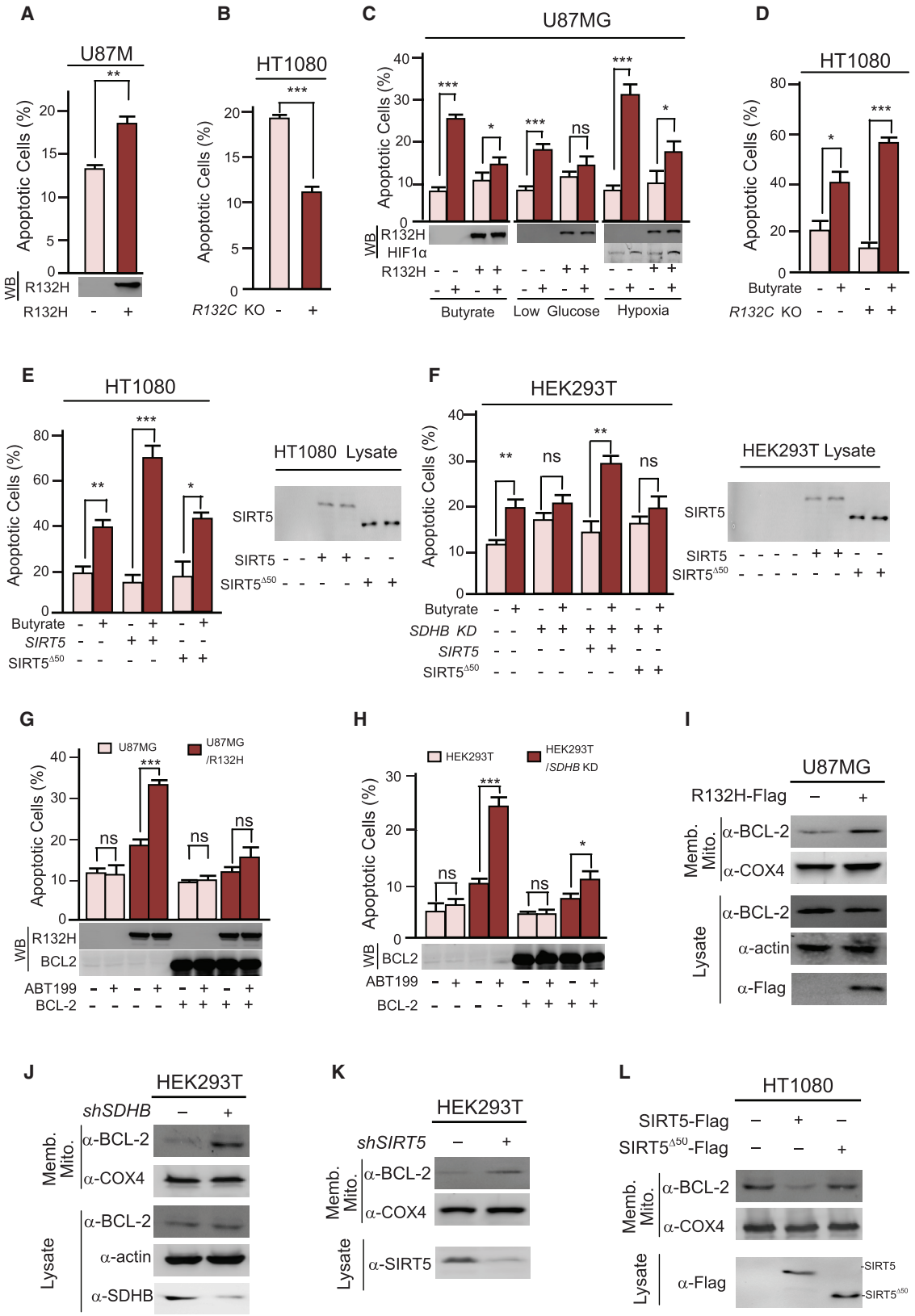

(legend on next page)

biosynthesis pathway. Therefore, glycine supplementation may facilitate removal of succinyl-CoA and inhibit succinylation. Indeed, hypersuccinylation induced by IDH1^{R132H} overexpression was successfully relieved by glycine supplementation (Figure 7E), and glycine supplementation not only lowered the cellular succinyl-CoA levels but also dose-dependently inhibited the hypersuccinylation caused by *SDHA* or *SDHB* knockdown (Figure 7F). Moreover, the OCR of HT10180 cells was increased upon treatment with glycine (Figure 7G). Furthermore, HT1080 xenografts from mice fed 5% glycine chow not only were 67% smaller (Figure 7H) but were also lower succinylated (Figure S7A) than those fed with normal chow. These data all confirmed that inhibiting succinylation blocked the oncogenic growth of HT1080 cells.

DISCUSSION

In the current study, we demonstrated that *IDH1/2* mutation-produced R-2HG promotes tumorigenesis through inducing hypersuccinylation-promoted cancerous metabolism and apoptosis resistance (Figure 7I). Deregulation of a single oncometabolite such as R-2HG has the same outcomes as those of multiple genes mutations to accomplish cancer transformation (Koivunen et al., 2012). This makes pathological sense because deregulated metabolites can affect the functions of a number of proteins/pathways through either noncovalent binding or covalent modification (Li et al., 2013). Moreover, different from other spontaneous lysine modifications such as lysine homocysteinylation (Jakubowski et al., 2000), lysine succinylation causes mitochondrial stress, since succinyl-CoA is produced inside the mitochondria. The preferred mitochondrial impairment by hypersuccinylation explained that elevated levels of homocysteine thiolactone are associated with coronary artery and neural tube defects (Blom and Smulders, 2011), while elevated succinyl-CoA levels are cancerous. Furthermore, deficiencies in FH or SDH are associated with lactic acidosis (Jaberi et al., 2013; Zinn et al., 1986); a mutation in any one of the four yeast SDH genes leads to loss of SDH function and an inability to grow by respiration (Lemire and Oyedotun, 2002), supporting that SDH inactivation induces cancerous metabolism.

IDH1/2 mutation-induced hypersuccinylation imposes stresses to mitochondria and triggers apoptosis resistance in *IDH1/2* mutation-harboring cells by promoting antiapoptotic protein BCL-2 to the membrane of the mitochondria, an event known to promote tumorigenesis (Igney and Krammer, 2002). It is worth noting that the recruitment of BCL-2 to the mitochondrial membrane not only provides a tumor-promoting mechanism for *IDH1/2* mutations but also may account for the unexplained observations that patients with *IDH* mutant-associated gliomas actually have a better prognosis (Ogura et al., 2015; Sabha et al., 2014; Sanson et al., 2009), as BCL-2 was found to be an independent indicator of favorable prognosis in early-stage breast cancer (Dawson et al., 2010) and in ovarian carcinoma (Herod et al., 1996). The tumorigenic mechanism of hypersuccinylation described above may also apply to *SDH* and *FH* mutations, as inactivation of SDH led to hypersuccinylation, and papillary 2 renal cell carcinoma samples with *FH* mutations were hypersuccinylated (Figure S7B, Table S3).

SIRT5 overexpression reversed cancerous metabolism and apoptosis resistance induced by *IDH1*^{R132H}-expressing or *SDH* inactivation, highlighted the tumor-suppressor role of the desuccinylase SIRT5, and was consistent with the downregulation of SIRT5 observed in squamous cell carcinoma (Lai et al., 2013). SIRT5 was also found to play oncogenic roles in lung carcinoma cells, potentially via activation of SOD1 and/or NRF2 (Lin et al., 2013; Lu et al., 2014). These, together with that relief of hypersuccinylation by either SIRT5 overexpression or glycine supplementation, resulted in inhibited growth of hypersuccinylated tumors, and shed light on alternative intervening approaches for *IDH1/2*, *SDH*, and *FH* mutation-related cancers.

EXPERIMENTAL PROCEDURES

Enzymatic Assays

Previously established methods were adopted for assays for metabolic enzymes. Detailed protocols are provided in the Supplemental Information.

Figure 6. Hypersuccinylation Recruits BCL-2 to the Mitochondria Membrane and Induces Apoptosis Resistance

(A and B) The percentages of apoptotic cells of U87MG and *IDH1*^{R132H}-expressing U87MG cells (A), HT1080, and *IDH1*^{R132C}-knockout HT1080 cells (B) were detected by flow cytometry (n = 3, error bars, ± SD).

(C) The percentages of apoptotic U87MG and *IDH1*^{R132H}-expressing U87MG cells were detected (n = 3; error bars, ± SD) under the absence and presence of sodium butyrate (5 mM, left), under normal (25 mM) and low (1 mM) glucose (middle) in the culture media and the absence and presence of hypoxia treatments (right).

(D) The percentages of apoptotic HT1080 and *IDH1*^{R132C}-knockout HT1080 cells were detected under the absence and presence of sodium butyrate (5 mM) in the culture media (n = 3; error bars, ± SD).

(E and F) The percentages of apoptotic HT1080 cells, *SIRT5*- and *SIRT5*$^{\Delta 50}$-expressing HT1080 cells (E), and HEK293T and *SDHB*-knockdown HEK293T, *SIRT5*- and *SIRT5*$^{\Delta 50}$-expressing *SDHB* knockdown HEK293T cells (F) under the absence and presence of sodium butyrate (5 mM) in the culture media (n = 3; error bars, ± SD).

(G) The percentages of apoptotic U87MG, BCL-2-expressing U87MG, *IDH1*^{R132H}-expressing U87MG, and BCL-2- and *IDH1*^{R132H} coexpressing U87MG cells under the absence and presence of ABT-199 (5 μM) in the culture media were measured (n = 3; error bars, ± SD).

(H) The percentages of apoptotic HEK293T and SDHB knockdown HEK293T cells that were and were not expressing BCL-2 were measured under the absence and presence of ABT-199 (n = 3; error bars, ± SD).

(I and J) BCL-2 levels in the lysate and in the mitochondrial membrane of U87MG and *IDH1*^{R132H}-expressing U87MG cells (I), and HEK293T and *SDHB*-knockdown HEK293T cells (J) were detected by western blot.

(K) BCL-2 levels in the mitochondria membrane of HEK293T and *SIRT5*-knockdown HEK293T cells.

(L) BCL-2 levels in the mitochondria membrane of HT1080, *SIRT5*- and *SIRT5*$^{\Delta 50}$-expressing HT1080 cells were determined.

See also Figure S6.

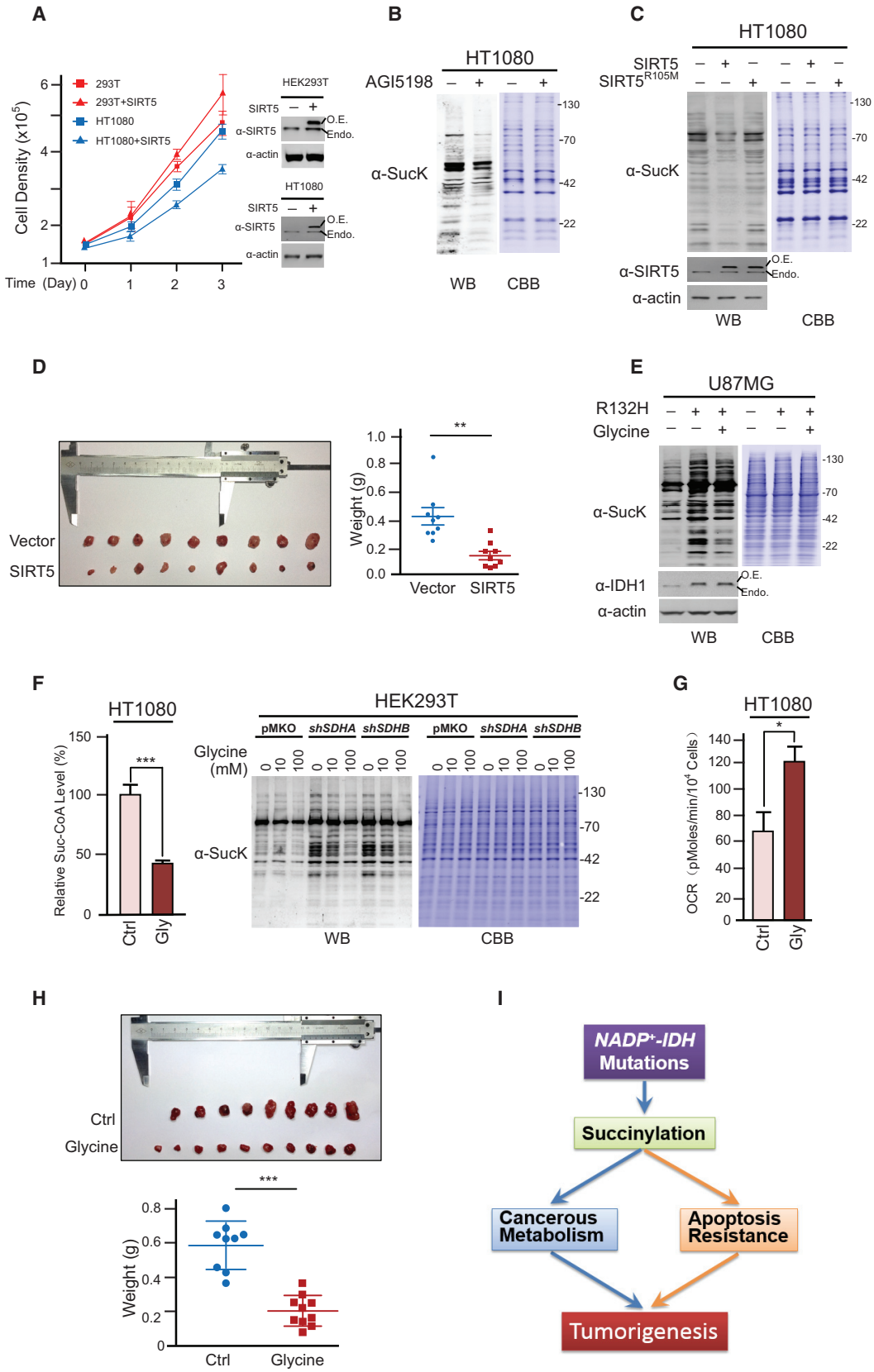

(legend on next page)

Cell Respiration Assays

Primary mice hepatocytes or HT1080 cells were seeded into XFe24 Cell Culture Microplates. Basal OCR; OCRs under treatments of oligomycin, FCCP, and rotenone; and antimycin A were each determined.

GC-MS Analysis

Metabolites were derivatized by methoxyamine hydrochloride before GC-MS analysis. Succinyl-CoA was converted to succinate before being subjected to GC-MS analysis.

Immunohistochemistry and Immunofluorescence

Succinylation was probed by α-SucK, mitochondria was probed by α-Mito, and mitochondrial membrane potential was probed by JC1. Tissue sections were prepared from formalin-fixed, paraffin-embedded specimens. Standard IHC procedures were followed. For immunofluorescence, permeabilized cells samples and tissue samples were blocked with 3% BSA, followed by incubation with primary and secondary antibodies and mounting samples with vecta shield mounting medium. Images were obtained on confocal laser scanning microscope.

Apoptosis Analysis

FITC Annexin V Apoptosis Detection Kit 1 (BD) was used to detect the apoptotic cells. Data were collected on Accuri C6 flow cytometer (BD Biosciences).

Human Samples and Animal Rights

Human samples were acquired from Fudan University Shanghai Cancer Center and the Affiliated Hospital of Guiyang Medical College with informed consent from the patients. The procedures related to human samples and animal manipulations were approved by Ethics Committee or Animal Welfare Committee of Fudan University.

Xenografts

HT1080 cells or HT1080 cells stably overexpressing SIRT5 were heterotransplantated into the Balb/C nude mice subcutaneously. The mice were maintained under conditions as specified, and the xenografts were obtained, weighted, and further analyzed for other properties.

Statistics

Pooled results were expressed as mean ± SD or SEM. Comparisons between groups were made by unpaired two-tailed Student's t test. Differences were considered statistically significant if p value was smaller than 0.05. Significance was indicated as $*p < 0.05$, $**p < 0.01$, and $***p < 0.001$.

ACCESSION NUMBERS

Microarray data of this study are available at Gene Expression Omnibus (GEO) repository under accession number GSE73662.

SUPPLEMENTAL INFORMATION

Supplemental Information includes seven figures, three tables, and Supplemental Experimental Procedures and can be found with this article at http://dx.doi.org/10.1016/j.molcel.2015.10.017.

AUTHOR CONTRIBUTIONS

S.Z. and W.X. conceived and planned the project and wrote the manuscript. F.L., X.H., C.H., Y.L., S.X., L.H., C.Y., H.Y., and F.W. executed molecular biological and animal experiments. X.H., L.L., and C.Y. analyzed metabolites; X.W., W.X., and J.Z. supervised animal experiments. D.Y., J.L., J.S., X.H., and Y.Q. collected cancer samples and performed IHC analysis. All authors read and discussed the manuscript.

ACKNOWLEDGMENTS

We thank MCB lab of Fudan University for providing HT1080 *IDH1*^{R132C} knockout cell line. This work was supported by the State Key Development Programs (973) of Basic Research of China (numbers 2012CB910103, 2013CB531200, 2013CB945401, 2013CB911204, 2015CB943300, and 2015AA020913), grants from the National Science Foundation of China (numbers 31330023, 81301717, and 81471454), International Cooperative grant from Minister of Science and Technology (2014DFA30630), and Science and Technology Municipal Commission of Shanghai (numbers 12ZR1440800 and 14ZR1402000).

Received: April 27, 2015
Revised: August 7, 2015
Accepted: October 9, 2015
Published: November 12, 2015

REFERENCES

Adam, J., Hatipoglu, E., O'Flaherty, L., Ternette, N., Sahgal, N., Lockstone, H., Baban, D., Nye, E., Stamp, G.W., Wolhuter, K., et al. (2011). Renal cyst formation in Fh1-deficient mice is independent of the Hif/Phd pathway: roles for fumarate in KEAP1 succination and Nrf2 signaling. Cancer Cell *20*, 524–537.

Amary, M.F., Bacsi, K., Maggiani, F., Damato, S., Halai, D., Berisha, F., Pollock, R., O'Donnell, P., Grigoriadis, A., Diss, T., et al. (2011). IDH1 and IDH2 mutations are frequent events in central chondrosarcoma and central and periosteal chondromas but not in other mesenchymal tumours. J. Pathol. *224*, 334–343.

Bennett, B.D., Kimball, E.H., Gao, M., Osterhout, R., Van Dien, S.J., and Rabinowitz, J.D. (2009). Absolute metabolite concentrations and implied enzyme active site occupancy in Escherichia coli. Nat. Chem. Biol. *5*, 593–599.

Figure 7. Inhibiting Hypersuccinylation Restores Mitochondrial Functions and Inhibits the Oncogenic Growth of *IDH1*^{R132C} Mutation-Bearing Cells

(A) Growth curves of HT1080 (blue) and HEK293T (red) cells with or without SIRT5 overexpression (left). The expression of SIRT5 in cells was confirmed (right). Error bars, ± SEM.

(B) Succinylation levels of HT1080 cells treated or not treated by AGI5198 were determined.

(C) Succinylation levels of HT1080 and SIRT5- or SIRT5^{R105M}-overexpressing HT1080 cells were compared.

(D) HT1080 cells and HT1080 cells stably overexpressing SIRT5 were used to generate xenografts in Balb/C nude mice. Xenografts of control and SIRT5-expressing HT1080 cells (left) and their weights (right) are shown. Error bars, ± SEM.

(E) Succinylation levels of U87MG, R132H-expressing U87MG and glycine treated R132H-expressing U87MG cells were compared.

(F) The succinyl-CoA level of HT1080 cells (left, glycine = 100 mM) and the succinylation levels (right) of control, and *SDHA* and *SDHB* knockdown HEK293T cells at the indicated glycine levels were determined.

(G) Oxygen consumption rates (OCR) of HT1080 cells and 100 mM glycine-treated HT1080 cells (n = 4; error bars, ± SD) were determined.

(H) Balb/C nude mice subcutaneously injected with HT1080 cells were fed normal chow or 5% glycine-supplemented chow ad libitum. The sizes (upper) and weights (down) of the xenografts generated from the two groups of mice are shown. One control mouse died during the experiment. Error bars, ± SEM.

(I) Schematic diagram of the proposed mechanism by which *IDH1/2* mutations promote tumor growth.

See also Figure S7.

Blom, H.J., and Smulders, Y. (2011). Overview of homocysteine and folate metabolism. With special references to cardiovascular disease and neural tube defects. J. Inherit. Metab. Dis. *34*, 75–81.

Chan, S.M., Thomas, D., Corces-Zimmerman, M.R., Xavy, S., Rastogi, S., Hong, W.J., Zhao, F., Medeiros, B.C., Tyvoll, D.A., and Majeti, R. (2015). Isocitrate dehydrogenase 1 and 2 mutations induce BCL-2 dependence in acute myeloid leukemia. Nat. Med. *21*, 178–184.

Christensen, B.C., Smith, A.A., Zheng, S., Koestler, D.C., Houseman, E.A., Marsit, C.J., Wiemels, J.L., Nelson, H.H., Karagas, M.R., Wrensch, M.R., et al. (2011). DNA methylation, isocitrate dehydrogenase mutation, and survival in glioma. J. Natl. Cancer Inst. *103*, 143–153.

Colak, G., Xie, Z., Zhu, A.Y., Dai, L., Lu, Z., Zhang, Y., Wan, X., Chen, Y., Cha, Y.H., Lin, H., et al. (2013). Identification of lysine succinylation substrates and the succinylation regulatory enzyme CobB in Escherichia coli. Mol. Cell. Proteomics *12*, 3509–3520.

Dang, L., White, D.W., Gross, S., Bennett, B.D., Bittinger, M.A., Driggers, E.M., Fantin, V.R., Jang, H.G., Jin, S., Keenan, M.C., et al. (2009). Cancer-associated IDH1 mutations produce 2-hydroxyglutarate. Nature *462*, 739–744.

Dawson, S.J., Makretsov, N., Blows, F.M., Driver, K.E., Provenzano, E., Le Quesne, J., Baglietto, L., Severi, G., Giles, G.G., McLean, C.A., et al. (2010). BCL2 in breast cancer: a favourable prognostic marker across molecular subtypes and independent of adjuvant therapy received. Br. J. Cancer *103*, 668–675.

Du, J., Zhou, Y., Su, X., Yu, J.J., Khan, S., Jiang, H., Kim, J., Woo, J., Kim, J.H., Choi, B.H., et al. (2011). Sirt5 is a NAD-dependent protein lysine demalonylase and desuccinylase. Science *334*, 806–809.

Figueroa, M.E., Abdel-Wahab, O., Lu, C., Ward, P.S., Patel, J., Shih, A., Li, Y., Bhagwat, N., Vasanthakumar, A., Fernandez, H.F., et al. (2010). Leukemic IDH1 and IDH2 mutations result in a hypermethylation phenotype, disrupt TET2 function, and impair hematopoietic differentiation. Cancer Cell *18*, 553–567.

Grunstein, M. (1997). Histone acetylation in chromatin structure and transcription. Nature *389*, 349–352.

Harris, M.H., and Thompson, C.B. (2000). The role of the Bcl-2 family in the regulation of outer mitochondrial membrane permeability. Cell Death Differ. *7*, 1182–1191.

Herod, J.J., Eliopoulos, A.G., Warwick, J., Niedobitek, G., Young, L.S., and Kerr, D.J. (1996). The prognostic significance of Bcl-2 and p53 expression in ovarian carcinoma. Cancer Res. *56*, 2178–2184.

Hirschey, M.D., Shimazu, T., Goetzman, E., Jing, E., Schwer, B., Lombard, D.B., Grueter, C.A., Harris, C., Biddinger, S., Ilkayeva, O.R., et al. (2010). SIRT3 regulates mitochondrial fatty-acid oxidation by reversible enzyme deacetylation. Nature *464*, 121–125.

Igney, F.H., and Krammer, P.H. (2002). Death and anti-death: tumour resistance to apoptosis. Nat. Rev. Cancer *2*, 277–288.

Isaacs, J.S., Jung, Y.J., Mole, D.R., Lee, S., Torres-Cabala, C., Chung, Y.L., Merino, M., Trepel, J., Zbar, B., Toro, J., et al. (2005). HIF overexpression correlates with biallelic loss of fumarate hydratase in renal cancer: novel role of fumarate in regulation of HIF stability. Cancer Cell *8*, 143–153.

Jaberi, E., Chitsazian, F., Ali Shahidi, G., Rohani, M., Sina, F., Safari, I., Malakouti Nejad, M., Houshmand, M., Klotzle, B., and Elahi, E. (2013). The novel mutation p.Asp251Asn in the β-subunit of succinate-CoA ligase causes encephalomyopathy and elevated succinylcarnitine. J. Hum. Genet. *58*, 526–530.

Jakubowski, H., Zhang, L., Bardeguez, A., and Aviv, A. (2000). Homocysteine thiolactone and protein homocysteinylation in human endothelial cells: implications for atherosclerosis. Circ. Res. *87*, 45–51.

Jin, G., Pirozzi, C.J., Chen, L.H., Lopez, G.Y., Duncan, C.G., Feng, J., Spasojevic, I., Bigner, D.D., He, Y., and Yan, H. (2012). Mutant IDH1 is required for IDH1 mutated tumor cell growth. Oncotarget *3*, 774–782.

Killian, J.K., Kim, S.Y., Miettinen, M., Smith, C., Merino, M., Tsokos, M., Quezado, M., Smith, W.I., Jr., Jahromi, M.S., Xekouki, P., et al. (2013). Succinate dehydrogenase mutation underlies global epigenomic divergence in gastrointestinal stromal tumor. Cancer Discov. *3*, 648–657.

Koivunen, P., Lee, S., Duncan, C.G., Lopez, G., Lu, G., Ramkissoon, S., Losman, J.A., Joensuu, P., Bergmann, U., Gross, S., et al. (2012). Transformation by the (R)-enantiomer of 2-hydroxyglutarate linked to EGLN activation. Nature *483*, 484–488.

Lai, C.C., Lin, P.M., Lin, S.F., Hsu, C.H., Lin, H.C., Hu, M.L., Hsu, C.M., and Yang, M.Y. (2013). Altered expression of SIRT gene family in head and neck squamous cell carcinoma. Tumour Biol. *34*, 1847–1854.

Lemire, B.D., and Oyedotun, K.S. (2002). The Saccharomyces cerevisiae mitochondrial succinate:ubiquinone oxidoreductase. Biochim. Biophys. Acta *1553*, 102–116.

Letouzé, E., Martinelli, C., Loriot, C., Burnichon, N., Abermil, N., Ottolenghi, C., Janin, M., Menara, M., Nguyen, A.T., Benit, P., et al. (2013). SDH mutations establish a hypermethylator phenotype in paraganglioma. Cancer Cell *23*, 739–752.

Li, F., Xu, W., and Zhao, S. (2013). Regulatory roles of metabolites in cell signaling networks. J. Genet. Genomics *40*, 367–374.

Lin, Z.F., Xu, H.B., Wang, J.Y., Lin, Q., Ruan, Z., Liu, F.B., Jin, W., Huang, H.H., and Chen, X. (2013). SIRT5 desuccinylates and activates SOD1 to eliminate ROS. Biochem. Biophys. Res. Commun. *441*, 191–195.

Losman, J.A., Looper, R.E., Koivunen, P., Lee, S., Schneider, R.K., McMahon, C., Cowley, G.S., Root, D.E., Ebert, B.L., and Kaelin, W.G., Jr. (2013). (R)-2-hydroxyglutarate is sufficient to promote leukemogenesis and its effects are reversible. Science *339*, 1621–1625.

Lu, C., Ward, P.S., Kapoor, G.S., Rohle, D., Turcan, S., Abdel-Wahab, O., Edwards, C.R., Khanin, R., Figueroa, M.E., Melnick, A., et al. (2012). IDH mutation impairs histone demethylation and results in a block to cell differentiation. Nature *483*, 474–478.

Lu, W., Zuo, Y., Feng, Y., and Zhang, M. (2014). SIRT5 facilitates cancer cell growth and drug resistance in non-small cell lung cancer. Tumour Biol. *35*, 10699–10705.

Ma, S., Jiang, B., Deng, W., Gu, Z.-K., Wu, F.-Z., Li, T., Xia, Y., Yang, H., Ye, D., Xiong, Y., and Guan, K.L. (2015). D-2-hydroxyglutarate is essential for maintaining oncogenic property of mutant IDH-containing cancer cells but dispensable for cell growth. Oncotarget *6*, 8606–8620.

Maloyan, A., Sanbe, A., Osinska, H., Westfall, M., Robinson, D., Imahashi, K., Murphy, E., and Robbins, J. (2005). Mitochondrial dysfunction and apoptosis underlie the pathogenic process in alpha-B-crystallin desmin-related cardiomyopathy. Circulation *112*, 3451–3461.

Nelson, D.L., and Cox, M.M. (2008). Lehninger Principles of Biochimestry (Freeman).

Nishida, Y., Rardin, M.J., Carrico, C., He, W., Sahu, A.K., Gut, P., Najjar, R., Fitch, M., Hellerstein, M., Gibson, B.W., and Verdin, E. (2015). SIRT5 regulates both cytosolic and mitochondrial protein malonylation with glycolysis as a major target. Mol. Cell *59*, 321–332.

Ogura, R., Tsukamoto, Y., Natsumeda, M., Isogawa, M., Aoki, H., Kobayashi, T., Yoshida, S., Okamoto, K., Takahashi, H., Fujii, Y., and Kakita, A. (2015). Immunohistochemical profiles of IDH1, MGMT and P53: practical significance for prognostication of patients with diffuse gliomas. Neuropathology *35*, 324–335.

Ooi, A., Wong, J.C., Petillo, D., Roossien, D., Perrier-Trudova, V., Whitten, D., Min, B.W.H., Tan, M.H., Zhang, Z., Yang, X.J., et al. (2011). An antioxidant response phenotype shared between hereditary and sporadic type 2 papillary renal cell carcinoma. Cancer Cell *20*, 511–523.

Park, J., Chen, Y., Tishkoff, D.X., Peng, C., Tan, M., Dai, L., Xie, Z., Zhang, Y., Zwaans, B.M., Skinner, M.E., et al. (2013). SIRT5-mediated lysine desuccinylation impacts diverse metabolic pathways. Mol. Cell *50*, 919–930.

Parsons, D.W., Jones, S., Zhang, X., Lin, J.C., Leary, R.J., Angenendt, P., Mankoo, P., Carter, H., Siu, I.M., Gallia, G.L., et al. (2008). An integrated genomic analysis of human glioblastoma multiforme. Science *321*, 1807–1812.

Rardin, M.J., He, W., Nishida, Y., Newman, J.C., Carrico, C., Danielson, S.R., Guo, A., Gut, P., Sahu, A.K., Li, B., et al. (2013). SIRT5 regulates the mitochondrial lysine succinylome and metabolic networks. Cell Metab. *18*, 920–933.

Rohle, D., Popovici-Muller, J., Palaskas, N., Turcan, S., Grommes, C., Campos, C., Tsoi, J., Clark, O., Oldrini, B., Komisopoulou, E., et al. (2013). An inhibitor of mutant IDH1 delays growth and promotes differentiation of glioma cells. Science *340*, 626–630.

Sabha, N., Knobbe, C.B., Maganti, M., Al Omar, S., Bernstein, M., Cairns, R., Çako, B., von Deimling, A., Capper, D., Mak, T.W., et al. (2014). Analysis of IDH mutation, 1p/19q deletion, and PTEN loss delineates prognosis in clinical low-grade diffuse gliomas. Neuro-oncol. *16*, 914–923.

Sanson, M., Marie, Y., Paris, S., Idbaih, A., Laffaire, J., Ducray, F., El Hallani, S., Boisselier, B., Mokhtari, K., Hoang-Xuan, K., and Delattre, J.Y. (2009). Isocitrate dehydrogenase 1 codon 132 mutation is an important prognostic biomarker in gliomas. J. Clin. Oncol. *27*, 4150–4154.

Selak, M.A., Armour, S.M., MacKenzie, E.D., Boulahbel, H., Watson, D.G., Mansfield, K.D., Pan, Y., Simon, M.C., Thompson, C.B., and Gottlieb, E. (2005). Succinate links TCA cycle dysfunction to oncogenesis by inhibiting HIF-alpha prolyl hydroxylase. Cancer Cell *7*, 77–85.

Turcan, S., Rohle, D., Goenka, A., Walsh, L.A., Fang, F., Yilmaz, E., Campos, C., Fabius, A.W., Lu, C., Ward, P.S., et al. (2012). IDH1 mutation is sufficient to establish the glioma hypermethylator phenotype. Nature *483*, 479–483.

Wagner, G.R., and Payne, R.M. (2013). Widespread and enzyme-independent Nε-acetylation and Nε-succinylation of proteins in the chemical conditions of the mitochondrial matrix. J. Biol. Chem. *288*, 29036–29045.

Wang, P., Dong, Q., Zhang, C., Kuan, P.F., Liu, Y., Jeck, W.R., Andersen, J.B., Jiang, W., Savich, G.L., Tan, T.X., et al. (2013). Mutations in isocitrate dehydrogenase 1 and 2 occur frequently in intrahepatic cholangiocarcinomas and share hypermethylation targets with glioblastomas. Oncogene *32*, 3091–3100.

Weinert, B.T., Schölz, C., Wagner, S.A., Iesmantavicius, V., Su, D., Daniel, J.A., and Choudhary, C. (2013). Lysine succinylation is a frequently occurring modification in prokaryotes and eukaryotes and extensively overlaps with acetylation. Cell Rep. *4*, 842–851.

Xiao, M., Yang, H., Xu, W., Ma, S., Lin, H., Zhu, H., Liu, L., Liu, Y., Yang, C., Xu, Y., et al. (2012). Inhibition of α-KG-dependent histone and DNA demethylases by fumarate and succinate that are accumulated in mutations of FH and SDH tumor suppressors. Genes Dev. *26*, 1326–1338.

Xu, W., Yang, H., Liu, Y., Yang, Y., Wang, P., Kim, S.H., Ito, S., Yang, C., Wang, P., Xiao, M.T., et al. (2011). Oncometabolite 2-hydroxyglutarate is a competitive inhibitor of α-ketoglutarate-dependent dioxygenases. Cancer Cell *19*, 17–30.

Yan, H., Parsons, D.W., Jin, G., McLendon, R., Rasheed, B.A., Yuan, W., Kos, I., Batinic-Haberle, I., Jones, S., Riggins, G.J., et al. (2009). IDH1 and IDH2 mutations in gliomas. N. Engl. J. Med. *360*, 765–773.

Zamzami, N., Susin, S.A., Marchetti, P., Hirsch, T., Gómez-Monterrey, I., Castedo, M., and Kroemer, G. (1996). Mitochondrial control of nuclear apoptosis. J. Exp. Med. *183*, 1533–1544.

Zhang, Z., Tan, M., Xie, Z., Dai, L., Chen, Y., and Zhao, Y. (2011). Identification of lysine succinylation as a new post-translational modification. Nat. Chem. Biol. *7*, 58–63.

Zhao, S., Lin, Y., Xu, W., Jiang, W., Zha, Z., Wang, P., Yu, W., Li, Z., Gong, L., Peng, Y., et al. (2009). Glioma-derived mutations in IDH1 dominantly inhibit IDH1 catalytic activity and induce HIF-1alpha. Science *324*, 261–265.

Zhao, S., Xu, W., Jiang, W., Yu, W., Lin, Y., Zhang, T., Yao, J., Zhou, L., Zeng, Y., Li, H., et al. (2010). Regulation of cellular metabolism by protein lysine acetylation. Science *327*, 1000–1004.

Zinn, A.B., Kerr, D.S., and Hoppel, C.L. (1986). Fumarase deficiency: a new cause of mitochondrial encephalomyopathy. N. Engl. J. Med. *315*, 469–475.